

A Drive Circuit for Piezoelectric Devices with Low Harmonics Content

Shaul Ozeri¹, Doron Shmilovitz¹ Chua-Chin Wang²

¹Tel-Aviv University, Tel-Aviv, Israel,

²National Sun Yat-Sen University, Taiwan

Abstract—This paper presents a high frequency low harmonics content AC source consisted of two phase shifted resonant legs, suitable for driving piezoelectric devices such as those employed in ultrasound radiators. The inverter is characterized by high efficiency, low harmonic distortion, good dynamic response, and simplicity of load power control. Particularly low harmonic content is attained by the proper phase shift between the two inverter legs.

I. INTRODUCTION

Piezoelectric transducers are widely applied for the generation of ultrasonic waves, in various application fields. The transducers' performance is highly dependent on its electrical excitation, which must be properly designed and optimized [1-4]. Thus, the power driver energizing a piezoelectric device is a critical component in all ultrasound systems. Typically, drivers consist of two cascaded stages: a pre-regulator stage that regulates a DC voltage and an AC power amplifier whose output drives the transducer. The dual-stage configuration implies reduced efficiency, and limited dynamics (e.g. response to variations of power command). Furthermore, applications using ultrasound phased array, requiring multiple high-frequency AC sources with per element apodization, each pre-regulator stage increases the overall device size and cost.

In this paper we show a highly sinusoidal, single-stage, high frequency piezoelectric transducer source which consists of two resonant legs generating a nearly sinusoidal 1MHz output voltage that is directly applied to the piezoelectric device. The source is suitable for driving PZT elements as well as PVDF membranes.

II. MAIN CHARACTERISTICS OF THE AC SOURCE

Low distortion sinusoidal AC source

The electrical impedance model of PZT elements contains multiple RLC branches in parallel to a dielectric capacitor. Each RLC branch is associated with a resonant mechanical vibration mode. This model has been suggested by Butterworth Van Dyke [9] and is illustrated in Fig 1.

Fig. 2 illustrates the measured electrical impedance of a Fujicermics Z2T30D-W disc shape device made of C2 material, (measured by AP200 network analyzer). The device's multi-resonant nature may be noted (along with numerous spurious vibration modes).

Typically, piezoelectric elements are driven so as to vibrate only at their fundamental vibration frequency,

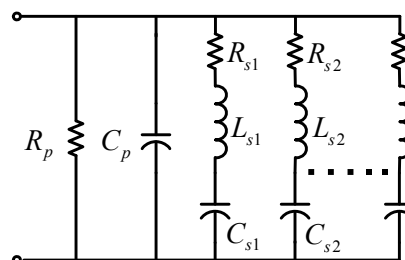


Fig. 1. The Butterworth Van Dyke model of PZT devices

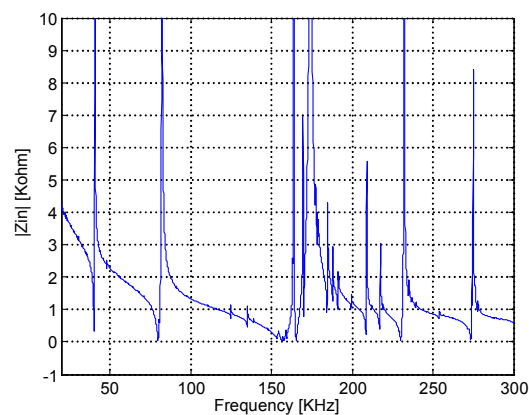


Fig. 2. Input impedance of a Z2.9N10.8x40R E PT measured by an AP-200 network analyzer

where the highest efficiency is attained. Furthermore, acoustical matching layer is usually incorporated to maximize the power transfer from the PZT elements to the media. Matching layers have a narrow operation bandwidth, in which the transfer coefficient is at its maximum value. Furthermore, excitation of piezoelectric elements by distorted signals might excite undesired vibration modes, such as higher harmonics of the fundamental, or transverse or shear vibration modes rather than longitudinal mode, which usually do not contribute to the desired effect, and only increase the power consumption. Thus, the *ac* excitation source is required to be highly sinusoidal, having low harmonic contents. The proposed inverter topology resembles the parallel resonant inverter topology, [10, 11], (chosen due to its high voltage gain); see Fig. 3. Capacitor C_r and inductor L_r constitute the resonant tank. The switches generate a positive 50% duty cycle square wave voltage, v_a , with a $V_s/2$ dc level, that is applied to the resonant tank. The dc offset is the result of not having a capacitive

voltage divider across the source as a conventional parallel resonant inverter would have (thus avoiding two electrolytic capacitors and the associated voltage balancing problem). The resulting resonant tank current is sinusoidal with a frequency equal to the switching frequency f_s . The capacitor voltage, v_b , is also sinusoidal, with the same frequency, but it contains a dc level as well. Thus, a series capacitor C_s was added in order to block this dc level, resulting in a pure sinusoidal voltage, v_L , at the load. The following assumptions are made in order to simplify the analysis: *a)* the resonant tank has a high enough quality factor, Q , and the switching frequency, f_s , is close enough to the resonance frequency, f_r , to allow only the first harmonic (and a dc component) to develop across C_r *b)* at the switching frequency, the series capacitor, C_s , has an impedance that is much lower than that of the resonant tank elements and that of the load so its effect on the ac component may be neglected (it only removes the dc level).

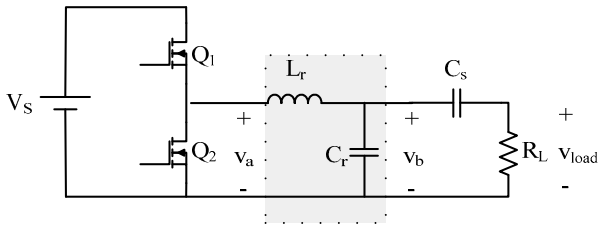


Fig. 3: The single ended inverter

These assumptions allow for the derivation of the simple model depicted in Fig. 4, where V_{a1} is the fundamental of the square wave v_{a1} (*dc* component removed) and V_{b1} is the fundamental of v_{b1} . Substituting $V_{a1}=2V_s/\pi$ yields the converter's gain:

$$\left| \frac{V_{b1}}{V_{a1}} \right| = \left| \frac{R_L \parallel (-jX_c)}{jX_L + (R_L \parallel (-jX_c))} \right|, \quad Q = \frac{\omega_0 L_r}{R_L}, \quad \omega_0 = \frac{1}{\sqrt{L_r C_r}}$$

AC source power control

Phase array piezoelectric ultrasound projectors, consists of multiple piezoelectric elements, each of them excited by a dedicated AC source. Each one of the *ac* sources is phase shifted (with respect to the other sources), and amplitude controlled (Apodization). The phase and amplitude control of the voltage signal that drives each element facilitates steering and focusing of the radiation lobe. This is typically accomplished by a two stage topology per each piezoelectric element. Since

a phased array system may include tens of piezoelectric elements, the overall circuitry required to independently excite each element is large. Furthermore, the dual power processing by the cascaded system implies reduced efficiency.

In the proposed ac source scheme, power control is implemented through the phase shifting the two inverter legs with respect to each other, resulting in a single stage that processes power. That results in reduced circuitry and increased efficiency, compared to regular implementations. The proposed bipolar inverter is shown in Fig. 6. The resulted voltage across the piezoelectric element is:

$$v_{load} = V_s \cdot \frac{8}{\pi} \cdot G(L_r, C_r) \cdot \sin\left(\frac{\varphi_1 - \varphi_2}{2}\right) \cdot \sin\left(2\pi f_s \cdot t + \frac{\varphi_1 + \varphi_2}{2}\right)$$

where G is the resonance tank transfer function, f_s , the switching frequency and φ_1 and φ_2 the phases of the square wave generated by leg #1 and leg #2 respectively. Evidently the voltage amplitude is defined through the phase difference between the two switching legs and the overall phase through the legs phases with respect to other ac sources in the array.

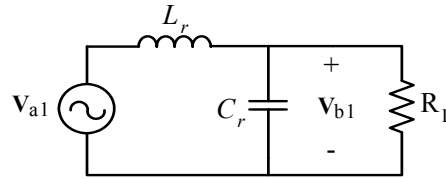


Figure 4: One leg basic model

III. SIMULATION RESULTS

The actual inverter proposed incorporates two legs as shown in Fig. 5. This allows for *a)* increasing the voltage gain and thus increasing the load power by a factor of up to 4 (if the two legs generate 180° out of phase signals) and *b)* control of the load voltage and power by programming the phase between the square waves generated by the two legs.

Furthermore, since the two signal that are present at the outputs of the two resonant tanks are quite similar a considerable amount of harmonics cancelation can be attained, depending on the phase shift between the two inverter legs.

The simulated circuit parameters are: $L_r=13.6\mu\text{H}$, $C_r=1.5\text{nF}$, $V_s=100\text{V}$ and $f_s=1\text{MHz}$.

Typical waveforms are shown in Fig. 6.

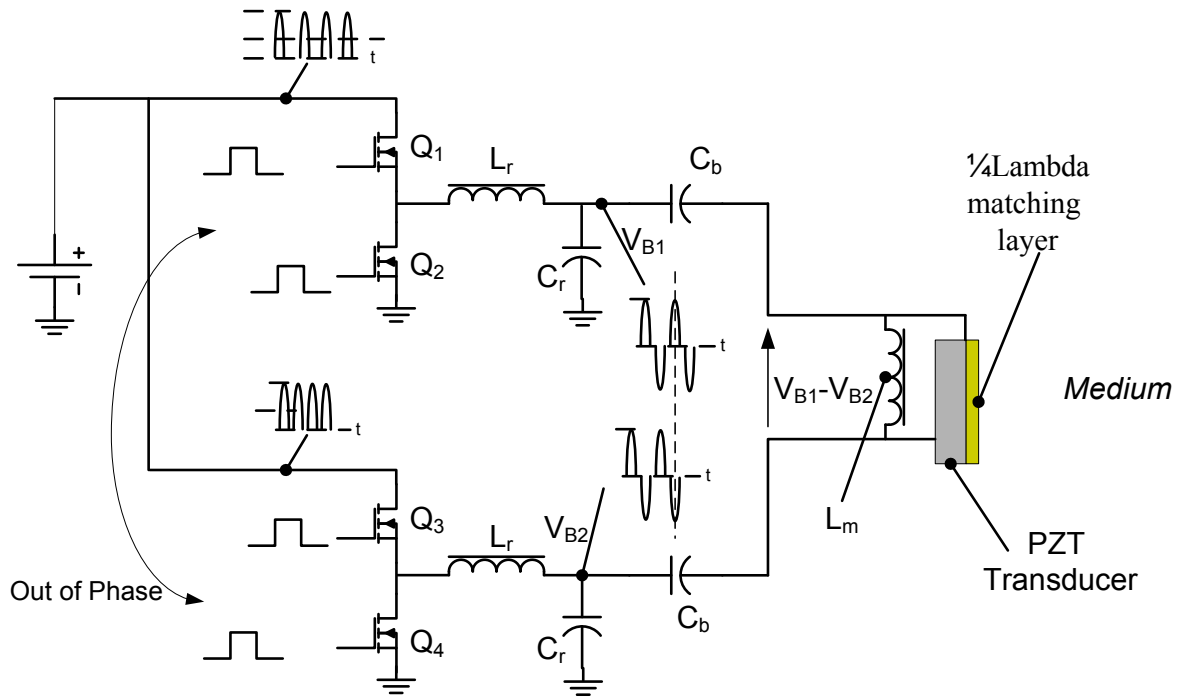


Fig. 5. The dual leg inverter scheme

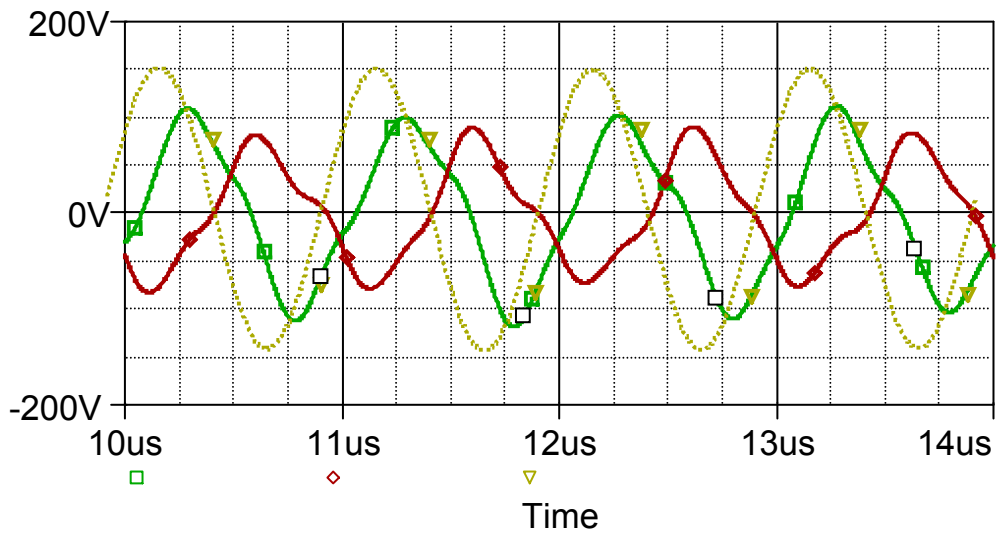


Fig. 6. Voltages at the outputs of the two resonant tanks (red and green) and across the piezoelectric load element (yellow)

So, in addition to generating low harmonic signal by using a resonant tank, an additional harmonics cancellation is attained due to the phase shift between the two signal, yielding a very low harmonics content in the voltage across the piezoelectric element. This is evident in Fig. 6: even though the individual legs voltages are somewhat distorted, the load voltage is seen to be highly sinusoidal.

Harmonics cancelation mechanism

The harmonics cancelation mechanism due to the dual leg excitation is quite simple. Assume the two legs voltages are identical (except they are phase shifted with respect to one another). Applying these two signals to the piezoelectric load element constitutes a subtraction of one voltage from the other and therefore, a certain attenuation of harmonics, depending on the phase shift between the voltage signals. For instance, if the two voltage signal are time shifted by $T/5$ (T representing the voltage signal period), then the fifth harmonic appears with the same phase on both load terminals and therefore will cancel out.

The total harmonic distortion (THD) of the load voltage dependence on the delay of one signal with respect to the other is plotted in Fig. 7.

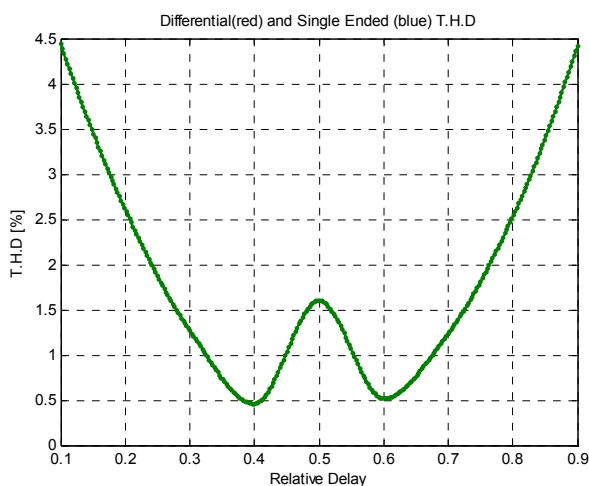


Fig. 7. THD of output voltage

Obviously this is a symmetrical graph around the $50\% \cdot T$ delay.

This function attains its minima around $0.4T$ and $0.6T$ which results from the fact that the third harmonic is the dominant one (to cancel it would require a delay of 333ns), and the 400ns represents a kind of weighted average for all the harmonics present in the signal.

Table I shows the normalized harmonics, one side and differential. The harmonic attenuation can be seen to be particularly effective at the third and fifth ones.

Table I

Harmonic number	Single ended	Differential voltage
1	1	1
2	1.12E-4	1.50E-03
3	7.23E-04	1.76E-01
4	1.88E-04	6.89E-04
5	2.88E-03	1.39E-02
6	1.62E-04	5.00E-04
7	1.16E-03	3.77E-03

IV. SUMMARY

A double sided resonant inverter suitable for piezoelectric devices drive is presented. The drive circuit has been proven to allow for control of the transducer's power in a large range of 10% to 100% (without using a pre-regulator). Power dynamics are fast and can be changed within $50\mu\text{s}$ or less. Typically, the generated waveforms exhibit low harmonic contents ($\text{THD} < 2\%$).

REFERENCES

- [1] A. Arnau, *Piezoelectric Transducers and Applications*, Springer-Verlag Berlin Heidelberg 2004
- [2] T. Ikeda, *Fundamentals of Piezoelectricity*, Oxford University Press, 1990.
- [3] S. Ben-Yaakov, G. Ivensky, "Drivers and rectifiers for piezoelectric elements", tutorial presented at PESC.05, June 2005.
- [4] S. Ben-Yaakov, N. Krihely, "Modelling and driving piezoelectric resonant blade elements", *IEEE APEC.04 Record*, pp. 1733-1739.
- [5] C. A. Rosen, "Ceramic Transformers and Filters", *Proceedings of Electronic Comp. Symp.*, 1956, pp. 205-211.
- [6] C. A. Rosen, US Patent No. 2,974,296, March 1961.
- [7] Anita M. Flynn, Seth R. Sanders, "Fundamental Limits on Energy Transfer and Circuit Considerations for Piezoelectric Transformers," *IEEE transactions on power electronics*, vol. 17, no. 1, January 2002, pp.8-14.
- [8] Sanchez A.M., Sanz M., Prieto R., Oliver J.A., Alou P., Cobos J.A., "Design of Piezoelectric Transformers for Power Converters by Means of Analytical and Numerical Methods," *IEEE transactions on industrial electronics*, vol. 55., no. 1, Jan. 2008, pp.79-88.
- [9] A. Arnau, Y. Jimenez, T. Sogorb "An extended Butterworth Van Dyke model for quartz crystal microbalance applications in viscoelastic fluid media", *IEEE Transactions on Ultrasonics, Ferroelectrics and Frequency Control*, Volume 48, Issue 5, Sept. 2001, pp. 1367 – 1382.
- [10] Robert W.Erickson & Dragan Maksimovic, *Fundamentals of Power Electronics*, second edition. Kluwer academic Publisher, 2001.
- [11] M. K. Kazimierzczuk & D. Czarkowski, *Resonant Power Converters*, John Wiley & Sons, 1995.